Numerical and analytical evaluation of airship configuration

A Golmakani[1]*, S Noori[1], N Karimi[2]
1. Amirkabir University of Technology, Tehran, Iran
2. Aerospace Research Institute, Iran

ABSTRACT
Today, airships have many uses and have been considered because they combine the benefits of a ship and an aircraft and the low cost of energy consumption. In this research, with the help of numerical solutions and analytical solutions in Datcom, three common configurations of an airship at various angles of attack are investigated. The results of numerical and analytical solutions are compared. Flow condition was considered at an altitude of 4 km above the ground. The same results are not obtained in numerical and analytical solutions. Certainly, numerical results can be cited more than analytical solutions because Datcom software has computational errors and has been simplified. It has been developed for the analytical flow solution on the slender body. However, despite the existing error, this software can be used to extract computational processes and sensitization some parameters. The results show that the approach of the tail fins to the tip of the airship increases the lift-to-drag ratio, and with increasing the length-to-diameter ratio, the aerodynamic performance also improves. In all variants, converting the fins to a cross-type variant improves the vehicle's aerodynamic performance.

1. INTRODUCTION

The history of the development of airships dates back to the 18th century. Nevertheless, the first documents about the design of airships date back to about 1941. A document released by the US Department of Warfare outlining the process of aerodynamic design, computing, and airship configuration. In this research, the relations are analytical, and computational and linearized relations have been used [1]. Solving the fluid flow on the airship in numerical form may seem simple, but it has many operational complexities. Due to its aerodynamic shape and wide surface, the airship often does not have fractures and sudden deformations on the fuselage surface. The surface changes in the fuselage are smooth and with a definite slope, causing the fluid flow to laminar flow, especially in the boundary layer. However, on the other hand, the long length of the vehicle, low speed, and not so high flight altitude cause the Reynolds number in the airship to be high, increasing the tendency of the flow to be turbulent. As a result, modeling and extracting the results of coefficients and forces on the vehicle in the wind tunnel cause problems due to high Reynolds. On the other hand, numerical solutions as engineering tools should be able to predict the flow behavior of the vehicle. For this purpose, various parameters such as the length and diameter of the airship will be important for the design team. A numerical simulation in China shows that increasing the length of the vehicle with the RANS model will increase the drag force. Flow separation is a factor in increasing the drag force, and this factor is directly related to the length of the vehicle.

*Corresponding Author: atosagolmakani@gmail.com

In other words, how the flow separates, and its location directly affects drag force, so length, diameter, and length-to-diameter ratio directly affect drag force due to changes in the separation area. Various calculations have shown that flow separation occurs at 70 to 80% of the vehicle length. When separation occurs later, the airship will experience more laminar flow on its body, which will reduce the drag force. Flow lines around the vehicle can distinguish the transition zone from laminar to turbulent flow. This method can provide an estimate of the separation area [2]. Examples of numerical solutions of fluid flow on the airship are used to calculate aerodynamic forces, including drag. In some of these examples, the vehicle's body is assumed to be rigid and numerical methods simulate fluid flow around the airship. Interaction of structure and fluid has been observed in some cases, but there is no need to consider forces and coefficients to calculate fluid flow around the vehicle. Also, due to the high surface level of the airship, considering details such as fins and some protrusions does not affect the calculation of the total drag force. The numerical solution of the flow around the airship carries challenges such as observing the physical phenomena of the flow. In a study in 2004, Kamal et al. [3] performed numerical simulations around an airship using various turbulence flow models. In this research, three turbulence flow models were used to observe the types of vortex-solving vehicles. The results show that the VMS-LES model has a better performance than the two models of k-ε and the turbulent flow model LES. In another example, Shields et al. [4] from the University of Virginia attempted to simulate the 1:75 scale version of an airship using a numerical method and extract the corresponding coefficients. This study shows that numerical solution does not provide an accurate answer in the calculation of lift force but can be effective for designing and extracting processes. In another study, Voloshin et al. [5] analyzed three turbulence flow models on an airship using numerical solutions. This study used some turbulence models such as k-ω, k-ε, and Spalart-Allmaras. The study results show that the Sparart-Allmaras turbulence flow model gives the best results compared to other models and experimental methods. In another study, Andan et al. [6] used a new solver to evaluate the aerodynamic characteristics of an airship. This research, which has been done as an analytical and experimental solution, shows that the flow separation on the airship is important and affects the stability status and coefficients of the vehicle. In addition, the effects of the dihedral angle of the fins and vertical tail on the aerodynamics of the airship have been investigated. Experimental research in the field of airships has also maintained its position. Ping et al. [7] calculated the coefficient and aerodynamic forces on a smaller scale in a wind tunnel using practical solutions in China. In this study, coefficients and forces were measured in different pitch and yaw angles in different situations, and the results of this study were compared with numerical solutions. A very important and key example has been found in articles and research that have been done on the effects of fin shape and its location. The article published in 2015 examines the types of fins on a fixed body and the effects of changes in the type and arrangement of the fins on the two coefficients of lift and drag. This numerical solution shows that the cross-type fin has a better aerodynamic performance than the two types of plus and conventional. The lift-to-drag ratio is optimal for it in the same way as other fins [8]. In 2019, Jefferson et al. [9] tried to calculate the coefficients and forces on the airship using numerical methods. This study shows that numerical solution validation using laboratory results obtained from wind tunnels is difficult. However, this solution will be acceptable for the initial phases and design. In their article, Alireza Akbari et al. [10] have numerically studied the damping coefficient of the roll of a conventional airship based on computational fluid dynamics. They used the numerical method and extracted the dynamic coefficient from Fluent software using MRF techniques.

Their results showed that this process's accuracy in calculating the roll's dynamic coefficients is very good compared to the reference numerical effects. In discussing the turbulence model, they observed that the Spalart-Allmaras is the best model for calculating the damping coefficient of the roll for their geometry. Another example of experimental work in this field was done in 2007 by Beheshti et al. [11]. They examined the drag of an airship experimentally. Sun et al [12] investigated the aerodynamic characteristics of a stratospheric airship in all stages of flight experimentally and numerically. The results showed that the head part plays a key role in the production of pitching and yawing moment, while the middle part plays an important role in the production of the rolling moment. The tail part is the main factor of the pressure drag force. During the flight, the contribution of the body (with the effect of the fins) to the aerodynamic drag force is dominant (more than 70%), and the fins contribute to the stable pitching moment. Slotnick [13] used numerical and experimental methods to calculate the forces acting on a high-lift aircraft. Investigating the separation of viscous flow in numerical and experimental solutions is one of the important goals of this research. Yueneng et al. [14] proposed a bionic method to design the aerodynamic shape of the airship inspired by physalia physalis. The calculation results showed that the designed stratospheric airship has better aerodynamic performance than the conventional stratospheric airship. Manikandan and Pant [15] checked various aspects of conceptual design and key issues including aerodynamics, dynamics, performance, thermal characteristics, structure, and optimization in the design of hybrid airships in detail in their review article. Ceruti et al. [16] optimized the configuration of an unconventional airship in a multidisciplinary way. The aim of optimization is to decrease the mass of the airship by maintaining the balance, reaching the design speed, and at the same time maintaining static longitudinal stability. He showed that the best surface-to-volume ratio is achieved with the sphere, although the greatest drag coefficient is attained with eccentric shapes. Liu et al. [17] compared the numerical results of the aerodynamic characteristics of the bare hull and the hull-fin configuration of an airship. A good agreement with the experimental results was observed in the aerodynamic coefficients and pressure distribution.

The airships are a member of the family of lighter-than-air aircraft, which fly because of being lighter than air [18]. Due to their configuration and the large reservoir of helium or hydrogen, they have a very high drag. Usually, they have slow cruising speeds that make the airship's aerodynamic design, including the shape of the surfaces, the length-to-diameter ratio, and the position of the tail fins, all exceptionally critical. On the other hand, one of the most important parameters in aerodynamic efficiency is decisive the flow separation zone at the end of the airship. Flow separation should be considered as a significant parameter in the aerodynamic forces, so the position of the tail fins and the plan of the empennage of the aircraft will be extremely significant [19].

In the present article, an attempt has been made to solve the fluid flow around an airship in different configuration models using numerical and analytical solutions and compare the results of these two solutions. According to what was thought, the results show that a numerical solution is more efficient than an analytical solution. Using the numerical solution, the physics of fluid flow and how the flow end of the vehicle is separated can be studied more carefully. This research has also tried to study the flow physics in this area with higher accuracy by analyzing the fluid flow behavior and the flow details around the airship.

2. DIFFERENT CONFIGURATIONS OF THE AIRSHIP

There are different parameters for airship modeling, but the most important parameter is the volume of the airship's envelope. With this parameter, other parameters of the airship such as hull diameter, hull length, location of the fins, and general external configuration can be extracted. In the present study, the volume of the airship's envelope is 27,000 m3. For this purpose, three different configurations have been considered and shown in Fig. 1, Fig. 2, and Fig. 3. The specifications of the three variants are given in Table 1. Configuration modeling has been done using Gambit software. The differences between configurations are in fitness ratio, the number of fins, fin length, and location. The effects of the fins' type, number, and arrangement on the flow behavior and various parameters will be examined with these three configurations. It should be noted that the gondola of the airship is not modeled in this simulation, and only the airship with the fins is modeled.

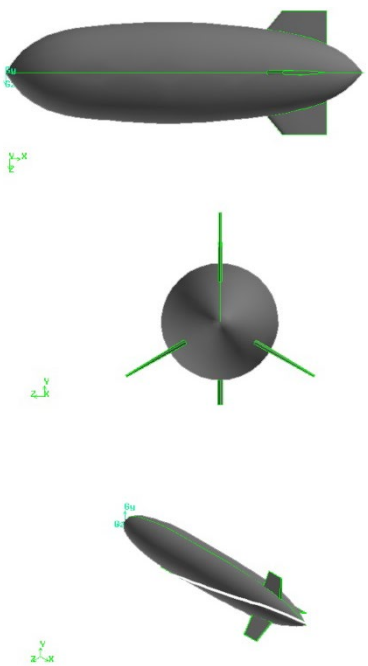

Fig. 1. Variant number one

Table 1. Configuration specifications of three different airships

Variant	Length of the vehicle (m)	Maximum radius of the vehicle (m)	Place of the fin from the tip of the airship (m)
1	59.512	5.05	44.8
2	45.209	6.676	32.8
3	53.18	6.26	38.62

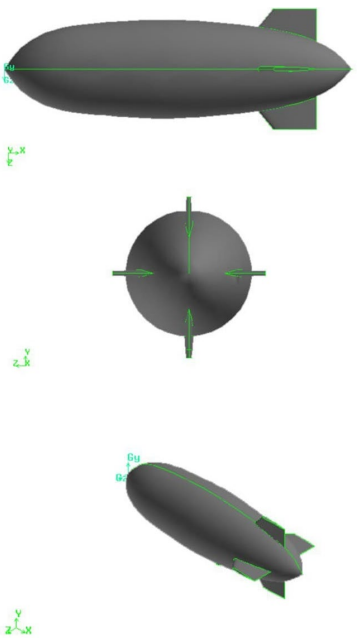

Fig. 2. Variant number two

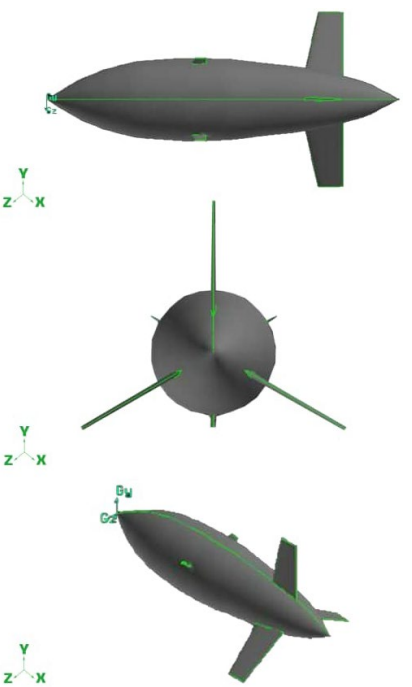

Fig. 3. Variant number three

3. GOVERNING EQUATIONS

To solve the flow around the airship, a numerical method has been used. In this regard, the Navier-Stokes equations have been solved, and due to the turbulence flow, the simplified form of these equations is given. The areas near the wall and the boundary layer are important and must be carefully resolved to study the aerodynamic coefficients. The two equations turbulence model k-ω SST, the aggregate of the k-ω and k-ε models, is used. It solves both the flow inside the boundary layer and close to the surface of the airfoil and the rest of the domain flow. The equation for conservation of mass, or continuity equation, might be written as equation (1):

$$\frac{\partial \rho}{\partial t} + \nabla \cdot (\rho \vec{v}) = S_m \tag{1}$$

Equation (1) is the common shape of the mass conservation, in which the source S_m is the mass delivered to the non-stop segment from the dispersed 2nd segment and any user-defined sources.

Conservation of momentum in an inertial (non-accelerating) reference outline is depicted by equation (2):

$$\frac{\partial}{\partial t}(\rho \vec{v}) + \nabla \cdot (\rho \vec{v} \vec{v}) = -\nabla p + \nabla \cdot (\bar{\tau}) + \rho \vec{g} + F \tag{2}$$

wherein p is the static pressure, $\bar{\tau}$ is the stress tensor, $\rho \vec{g}$ and F are the gravitational body force and external body forces, respectively. F furthermore incorporates different model-dependent supply phrases which include porous-media and user-described sources.

The stress tensor is given by equation (3):

$$\bar{\tau} = \mu \left[(\nabla \vec{v} + \nabla \vec{v}^T) - \frac{2}{3} \nabla \cdot \vec{v} I \right] \tag{3}$$

where μ is the molecular viscosity, I is the unit tensor, and the second term on the right-hand side is the effect of volume dilation [20].

The fluid flow in the present subject is solved based on the k-ε turbulence flow model. This turbulence model can provide suitable answers in subsonic and supersonic modes near the wall and free flow. Also, considering that the main goal of this paper is to calculate the coefficients and forces, especially the two lift and drag forces on the vehicle, this model can lead to appropriate answers [21].

Datcom software has also been used for the analytical solution. The basis of this software is solving linear analytical equations [22]. The equations solved in this software are analytical.

4. NUMERICAL INVESTIGATION

Due to the low velocity of the flow in the airship, solving the fluid flow is very complicated. Therefore, the flow resolution settings on this device must be done with high accuracy.

4.1. Boundary condition

The flow solution for these airships occurred at an altitude of 4 km above sea level and a cruising speed of 40 km/h. Also, the maximum speed of the vehicle is 72 km/h. Because the flow is subsonic and the device's maximum speed is 72 km/h, more attention should be paid to the upstream flow in choosing the solution domain. For this purpose, the front of the solution domain is ten times the model length, and the back is the same value. Due to the symmetry configuration of the airship, to decrease the computational cost and flow resolution time, the symmetry boundary condition has been used in modeling the airship. For this purpose, the airship is divided in half from the middle, and the middle plane's symmetry boundary condition is considered. The solution domain was divided into two parts, upstream and downstream of the flow. The pressure outlet boundary condition and the downstream of the velocity inlet boundary condition were considered for the upstream of the flow. Due to the flight conditions of the airship, for the inlet boundary condition, the inlet velocity of the flow was considered 20 m/s. For the outlet pressure, the pressure of 4 km from the table of atmospheric conditions was considered.

4.2. Grid study

The computational domain for the three configurations is meshed by the unstructured grid. Under the set boundary conditions, the solution field and the configuration of the airship are halved, and only one-half of it meshes. Fig. 4 shows the computational domain grid of the flow. Fig. 5 shows the airship surface grid for variant 3.

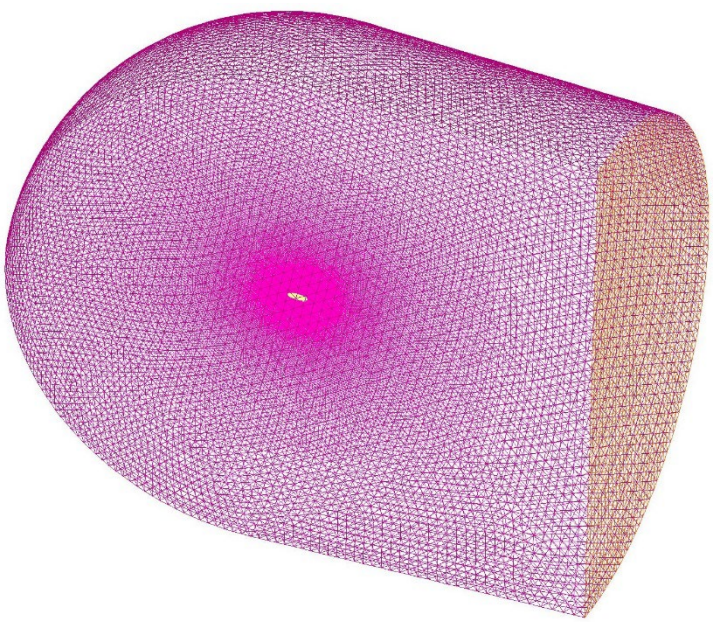

Fig. 4. Computational domain grid

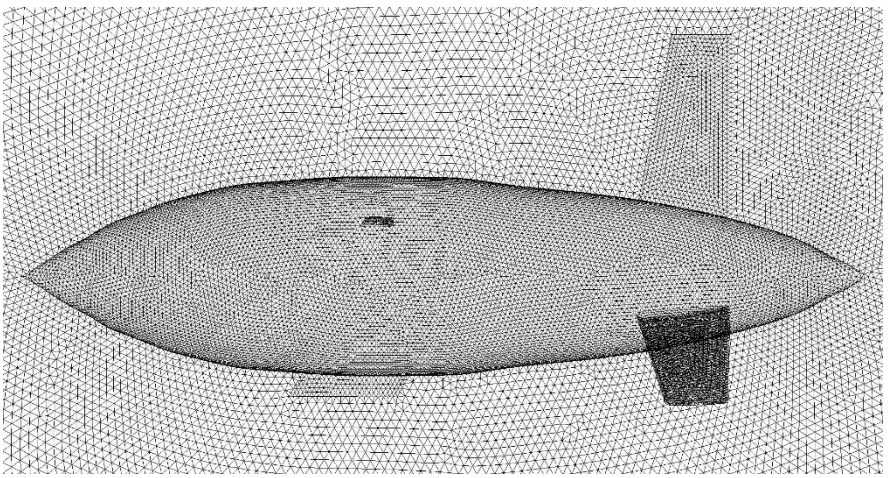

Fig. 5. Airship surface grid for variant 3

For all three variants, the grid resolution study has been performed, and the optimal grid has been selected to evaluate the results of flow solving. Examples of results related to grid-independent solution for variant one are given in Table 2. According to Table 2, a grid with 800,000 cells can be selected as the optimal grid because it has less than 2% error than a grid with more cells.

Table 2. Grid resolution study for variant 1

Number of cells	**CD**
300000	0.0093
600000	0.023
800000	0.0498
1200000	0.0501

4.3. Design of aerodynamic configuration

Aerodynamic analysis of airships includes different parts. Different parts of the airship must be analyzed from different perspectives to form the outer body. As a standard model for the aerodynamic design of the outer body of an airship, four parts of the body and nose design, fins and surfaces, design of the tails, and engine position are the main parts of the aerodynamic configuration of the airship. According to the studies, the fitness ratio is very important to the design of the configuration. This coefficient is a function of aerodynamic shape and symmetry streamlines to reduce drag, its most important indicator. In the airship design, the fitness ratio can be changed according to the constant volume of gas inside the envelope. It will be tried to select this coefficient according to the mission's requirements and the approach to reducing the aerodynamic drag force. In the design of the tails, considerations of flow vortices and reduction of the drag force are very important. Also, the vehicle's stability in maneuvers is the other important point in the design of the tails [23].

5. RESULTS AND DISCUSSION

One of the important parameters in aerodynamic simulation is the pressure coefficient and its distribution on the body surface. By comparing the pressure coefficient as a key parameter, the behavior of the flow, including the separation zone, can be estimated. For variant number one, with three fins, the pressure coefficient contours for the five and 10-degree angles of attack appeared in Fig. 6 and Fig. 7. Fig. 8 displays the velocity vectors about the vehicle at a 5-degree angle of attack. The convergence of the vectors at the end of the airship is clear in Figure.

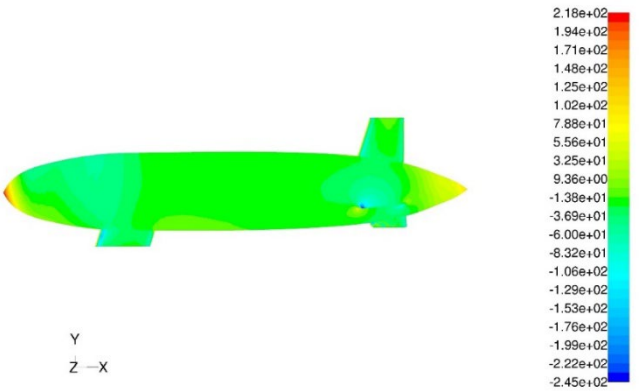

Fig. 6. Pressure coefficient on variant number one in the 5-degree angle of attack

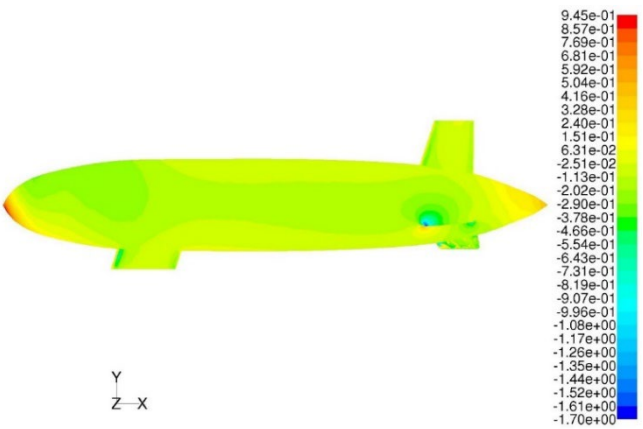

Fig. 7. Pressure coefficient on variant number one in the 10-degree angle of attack

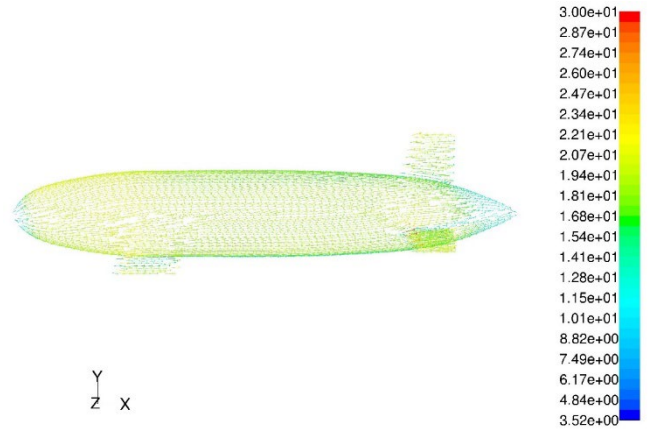

Fig. 8. Velocity vectors on variant number one in the 5-degree angle of attack

Enhancement of the angle of attack for variant number one increases the pressure at the end of the airship, especially after the tail. The pressure at the top of the airship creates a turbulent area behind the vehicle, which creates flow vortices and improves the condition of the lift to drag.

For variant number two, the effects of the angle of attack on the pressure coefficient distribution will be investigated. The pressure coefficient distribution on the end of the vehicle can determine the flow pattern in this area and the flow separation. Increased pressure in this area is normal due to the vortices at the end of the airship and the flow behind the fins. Figures 9, 10, and 11 show the pressure coefficient distribution on configuration two at different angles of attack.

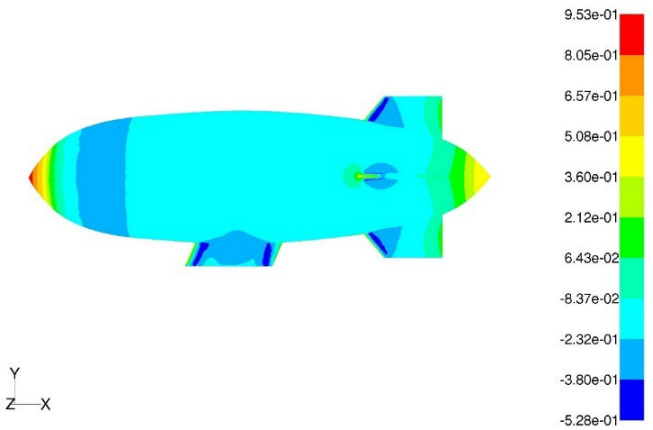

Fig. 9. Pressure coefficient on variant number two in zero degrees angle of attack

The pressure coefficient diagrams of variant 2 are visible at the end of the airship, behind the fins; with increasing angle of attack, the pressure coefficient increases and causes the flow pattern and its separation to occur in such a way that the lift-to-drag ratio increases.

The pressure coefficient distribution of variant three at various angles of attack is shown in Fig. 12, Fig. 13, and Fig. 14.

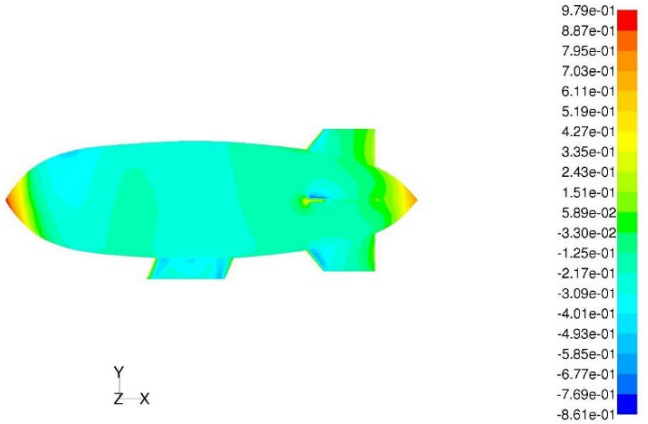

Fig. 10. Pressure coefficient on variant number two in the 5-degree angle of attack

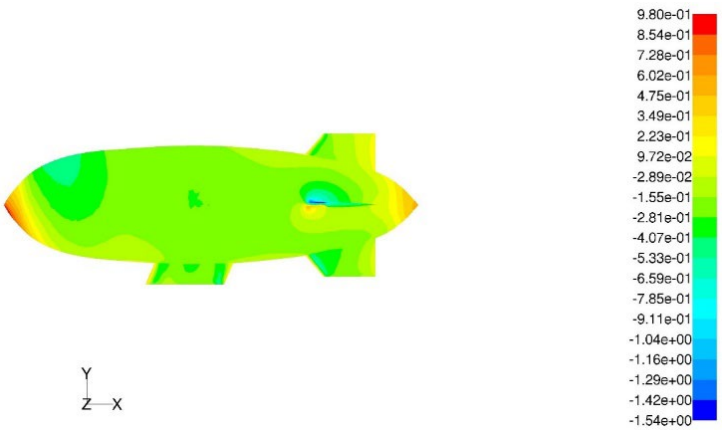

Fig. 11. Pressure coefficient on variant number two in the 10-degree angle of attack

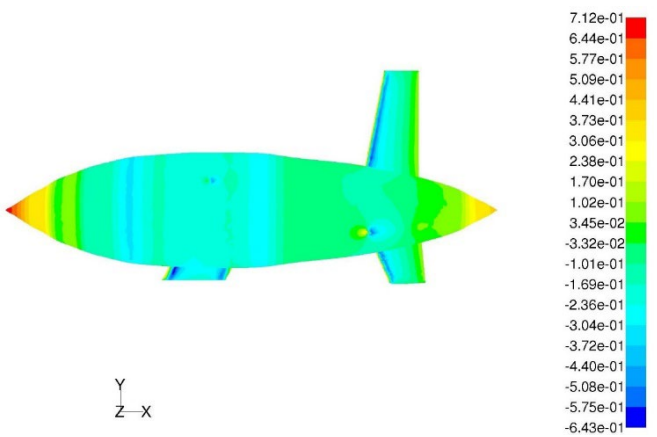

Fig. 12. Pressure coefficient on variant number three in zero degrees angle of attack

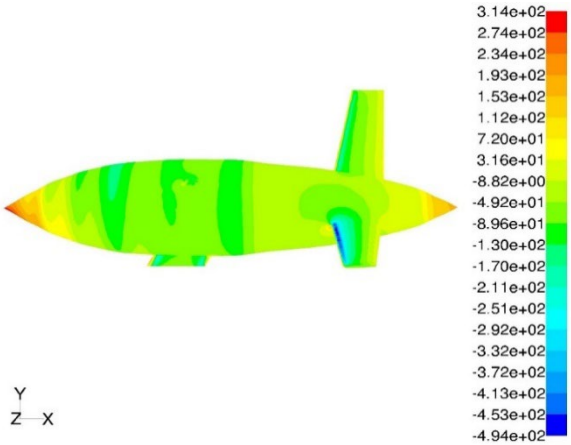

Fig. 13. Pressure coefficient on variant number three in the 5-degree angle of attack

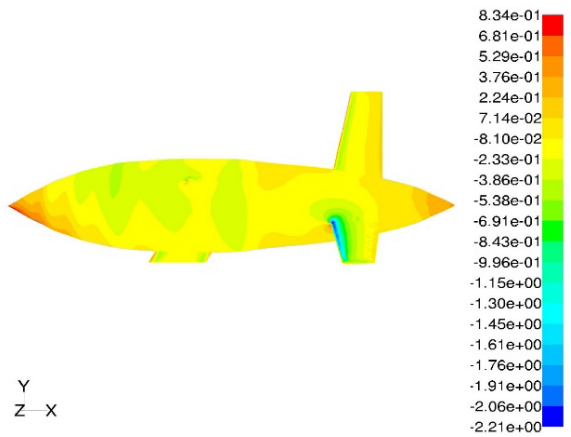

Fig. 14. Pressure coefficient on variant number three in the 10-degree angle of attack

6. VALIDATION

The numerical solution was performed in the flow condition in Peter Funk's article to validate the results of the numerical solution, and its outcomes were compared with the conclusion of the article [24]. The validation of the pressure coefficient is shown in Figures 15 and 16.

By Fig. 15 and Fig. 16, the conclusions display a very good settlement among the records, and the range of pressure coefficient with similar samples is in a certain range. Therefore, the numerical solution has good accuracy and is consistent with the experimental results.

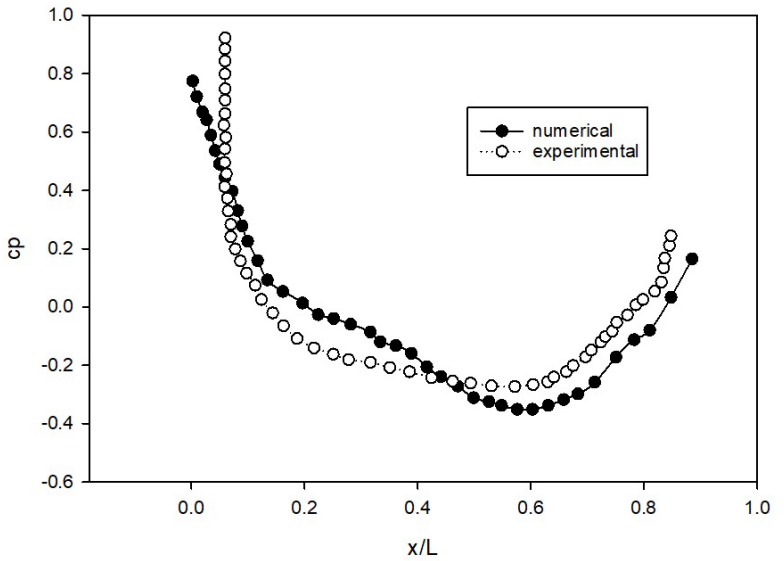

Fig. 15. Validation of pressure coefficient [24]

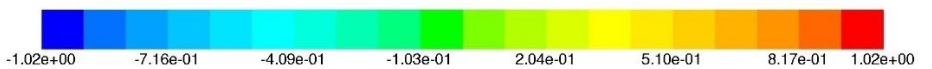

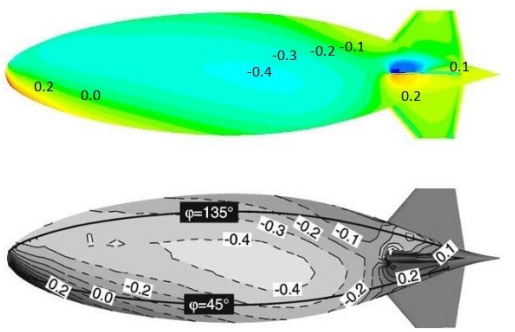

Fig. 16. Validation of distribution of pressure coefficient [24]

7. ANALYZE THE POSITION OF THE FINS ON THE FUSELAGE BY USING THE ANALYTICAL SOLUTION

One of the important things in many aerodynamic parameters of the airship is the position of the fins of the airship, the effect of which is determined on the aerodynamic coefficients by the effect on the separation of the flow. In this part of the research, using the Datcom analytical solver, the effects of separation of the flow at the end of the vehicle and its effect on the lift and drag coefficients for three variants will be presented. In this regard, in Table 3, Table 4, and Table 5, the effect of movement of the fin in the longitudinal direction of the vehicle for three variants in different angles of attack is given.

Table 3. Effect of movement of the fin on lift and drag in variant 1

Place of the fin from the tip of the airship (m)	**Angle of attack (degree)**	**Lift coefficient (CL)**	**Darg coefficient (CD)**	**CL/CD**
	0	0.0	0.073	0.0
40.8	5	0.367	0.104	3.534
	10	0.745	0.201	3.711
	0	0.0	0.074	0.0
44.8	5	0.352	0.103	3.414
	10	0.718	0.197	3.651
	0	0.0	0.074	0.0
48.8	5	0.328	0.101	3.246
	10	0.672	0.189	3.56

Table 4. Effect of movement of the fin on lift and drag in variant 2

Place of the fin from the tip of the airship (m)	**Angle of attack (degree)**	**Lift coefficient (CL)**	**Darg coefficient (CD)**	**CL/CD**
	0	0.0	0.089	0.0
28.8	5	0.209	0.106	1.97
	10	0.473	0.173	2.743
	0	0.0	0.089	0.0
32.8	5	0.201	0.106	1.901
	10	0.45	0.168	2.674
	0	0.0	0.089	0.0
36.8	5	0.182	0.104	1.752
	10	0.405	0.16	2.527

It can be seen that the lift-to-drag ratio increases by the forwarding movement of the fins. It can be expected that the forward movement of the fins will optimize aerodynamic behavior. There is a fundamental difference between the data obtained from variant three and variant one calculations: the proximity of the lift-to-drag ratio in the five and 10-degree angles of attack; this is due to the fin's increasing size and its effects. It can be expected that increasing the size of the fins will reduce the effects of the angle of attack. In examining the effects of the angle of attack, it can be seen that by increasing the angle of attack of the airship in each case, the lift-to-drag ratio increases, which is obvious and acceptable by considering the type of the configuration and the principles of flow resolution.

Table 5. Effect of movement of the fin on lift and drag in variant 3

Place of the fin from the tip of the airship (m)	Angle of attack (degree)	Lift coefficient (CL)	Darg coefficient (CD)	CL/CD
	0	0.0	0.076	0.0
34.62	5	0.41	0.109	3.75
	10	0.794	0.208	3.82
	0	0.0	0.076	0.0
38.62	5	0.393	0.108	3.638
	10	0.764	0.203	3.764
	0	0.0	0.076	0.0
42.62	5	0.371	0.106	3.494
	10	0.728	0.197	3.695

7.1. Investigation the effect of rotating the fins and converting them to the Cross-type

One of the important parameters in the configuration of the airships is selecting the type of fins and their installation angle to the horizontal axis of the vehicle. In the cross-type configuration, the mounting angle of the fins is 45 degrees to the horizon, and the fins are mounted in a star shape. For variants 1 and 3, while maintaining the cross-section of the fins, the three fins are changed to four fins and are installed crosswise; for variant two, the mounting angle of the fins relative to the horizon changes. The analytical solution results of changing the fins to cross-type are specified in Table 6, Table 7, and Table 8.

Table 6. Effect of changing fins to cross-type on lift and drag in variant 1

Place of the fin from the tip of the airship (m)	Angle of attack (degree)	CL/CD (Cross-type)	CL/CD (three fins)
	0	0.0	0.0
40.8	5	3.409	3.534
	10	3.678	3.711
	0	0.0	0.0
44.8	5	3.293	3.414
	10	3.614	3.651
	0	0.0	0.0
48.8	5	3.888	3.246
	10	3.889	3.560

According to Table 6, it can be seen that the conversion of three fins to four fins improves the lift-to-drag ratio when the position of the fins is shifted backward. According to Table 7 and Table 8, it can be seen that the conversion of the fins to the cross-type can improve the lift-to-drag ratio and aerodynamic efficiency in all places of installation of the fins. Changing the number of fins changes the separation behavior and consequently the lift and drag coefficients and increases the aerodynamic efficiency.

Table 7. Effect of changing fins to cross-type on lift and drag in variant 2

Place of the fin from the tip of the airship (m)	Angle of attack (degree)	CL/CD (Cross-type)	CL/CD (Plus-type)
	0	0.0	0.0
28.8	5	2.325	1.97
	10	2.98	2.743
	0	0.0	0.0
32.8	5	2.248	1.901
	10	2.892	2.674
	0	0.0	0.0
36.8	5	2.078	1.752
	10	2.732	2.527

Table 8. Effect of changing fins to cross-type on lift and drag in variant 3

Place of the fin from the tip of the airship (m)	Angle of attack (degree)	CL/CD (Cross-type)	CL/CD (three fins)
	0	0.0	0.0
34.62	5	4.371	3.75
	10	4.164	3.82
	0	0.0	0.0
38.62	5	4.254	3.638
	10	4.101	3.764
	0	0.0	0.0
42.62	5	4.097	3.494
	10	4.024	3.695

8. ANALYZE THE FITNESS RATIO BY USING THE ANALYTICAL SOLUTION

One of the airship configuration parameters is the fitness ratio, which directly affects the lift and drag coefficient of the vehicle. For this reason, in the three selected variants, the balconies and exterior surfaces, including the gondola, have been removed. Only the effect of fitness ratio on the vehicle has been investigated. The results of this case are given in Table 9.

Table 9. Effect of fitness ratio on lift and drag

Variant	Angle of attack (degree)	Fitness ratio (L/D)	CL/CD
	0		0.0
1	5	11.766	0.227
	10		0.912
	0		0.0
2	5	6.771	0.067
	10		0.405
	0		0.0
3	5	8.493	0.127
	10		0.607

Table 10. Compare the analytical and numerical solution

Variant	Angle of attack (degree)	C_L/C_D for the numerical solution	C_L/C_D for analytical solution	Error (%)
	0	0.01	0.0	1
1	5	2.26	3.414	51.06
	10	4.9	3.651	25.49
	0	0.001	0.0	1
2	5	1.86	1.901	2.2
	10	7.1	2.674	62.34
	0	0.001	0.0	1
3	5	4.1	3.638	11.27
	10	18.0	3.764	79.1

Table 9 shows that the lift-to-drag ratio decreases with the increasing diameter of the airship. Increasing the length to diameter is a positive parameter for an airship. Among the variants, variant 1, with the highest length-to-diameter ratio, has the best aerodynamic efficiency, and variant 2 has the worst condition.

The lift-to-drag ratio for the three selected variants for comparing the numerical solution with the analytical solution is given in table 10.

From Table 10, it can be understood that increasing the angle of attack will cause errors in the comparison between numerical and analytical solutions. As mentioned, the results of the numerical solution are more acceptable for this research. Among the selected variants, variant 3, due to the large fins, will have more errors in the higher angle of attack, which is shown in the table. However, the results show that variant number 3 has a higher lift-to-drag ratio than others.

9. CONCLUSIONS

In the present article, aerodynamic calculations have been performed on three selected airship configurations. The three selected configurations include three and four fins at different angles of attack. This research aims to find the selected configuration from aerodynamic performance to reduce the drag force and increase the lift force. Increasing the lift-to-drag ratio is the main goal of this research. For this purpose, the analytical solution was performed by Datcom software, and the numerical solution was performed. The numerical solution obtained the desired results, but Datcom software and an analytical solution were used to evaluate the changes in forces and coefficients. Dimensionless numbers, such as the lift-to-drag ratio, are the criteria for deciding on an analytical solution.

Due to computational constraints, symmetry boundary conditions have been used in numerical solutions. Also, an unstructured computational grid has been used to increase the density of cells near the body. Also, in the computational grid for each of the configurations, the independence of the grid is examined. The numerical solution is the type of turbulent flow, and the solution boundary conditions are adjusted based on the inlet speed and the outlet pressure according to the client's needs. What is certain and expected is that the same results are not obtained in numerical and analytical solutions. Certainly, numerical results can be cited more than analytical solutions because Datcom software has an inherent computational error and has been simplified.

Also, this software is mostly developed for analytical solutions to the flow of thin objects. However, despite the existing errors, this software can be used to extract computational processes and sensitization some parameters. The numerical and analytical solution results show that the lift-to-drag ratio is optimal in variants with smaller diameters. The numerical and analytical solutions show that the ratio of lift to drag is optimal in variants with a more fitness ratio, and with the increasing diameter as expected, drag force increases.

Another important result is the location of the fins behind the vehicle. In three variants, the fins' forward movement and the fins and the approach of the fins to the tip of the airship disrupt the layout of the flow at the end of the airship and delay the separation, improving the aerodynamic performance lift-to-drag ratio of the airship. On the other hand, the movement of the fins towards the end of the airship causes interference in the vortices flow and the flow behind the fins. Therefore, it is appropriate for the fins to move forward as much as possible from an aerodynamic point of view. Of course, this issue should also be considered from a systemic perspective, and the present study is only from the perspective of aerodynamics. Moreover, according to studies conducted among different fins, the cross-type will have the most excellent execution in terms of lift-to-drag ratio. In fact, in all variants, converting the fins from plus to cross or from the three-fins to four-cross fins improves the vehicle's aerodynamic performance.

REFERENCES

[1] Carrión M, Steijl R, Barakos G, Stewart D. Analysis of hybrid air vehicles using computational fluid dynamics. Journal of Aircraft. 2016;53(4):1001-12.

[2] Technical manual of airship aerodynamics, war department, February 1941. TM1-320.

[3] El Omari K, Schall E, Koobus B, Dervieux A. Turbulence modeling challenges in airship CFD studies. Monografías del SeminarioMatemáticoGarcía de Galdeano. 2004(31):545-54.

[4] Shields K. CFD applications in airship design. 2010.

[5] Voloshin V, Chen YK, Calay RK. A comparison of turbulence models in airship steady-state CFD simulations. arXiv preprint arXiv:12102970. 2012.

[6] Andan AD, Asrar W, Omar AA. Investigation of aerodynamic parameters of a hybrid airship. Journal of Aircraft. 2012;49(2):658-62.

[7] Liu P, Fu G-y, Zhu L-j, Wang X-l. Aerodynamic characteristics of airship Zhiyuan-1. Journal of Shanghai Jiaotong University (Science). 2013;18(6):679-87.

[8] Yanxiang C, Yanchu Y, Jianghua Z, Xiangqiang Z, editors. Numerical aerodynamic investigations on stratospheric airships of different tail configurations. 2015 IEEE Aerospace Conference; 2015: IEEE. 10.1109/AERO.2015.7118977

[9] Mendonça Junior JL, Santos JS, Morales MA, Goes LC, Stevanovic S, Santana RA, editors. Airship aerodynamic coefficients estimation based on computational method for preliminary design. AIAA Aviation 2019 Forum; 2019.

[10] Noori S, Akbari A, Spahvand P. A numerical investigation on the roll damping coefficient of a typical airship based on the computational fluid dynamics. Journal of Aerospace Science and Technology. 2021;14(2).

[11] Beheshti B, Soller A, Wittmer F, Abhari R, editors. Experimental investigation of the aerodynamic drag of a high altitude airship. 7th AIAA ATIO Conf, 2nd CEIAT Int'l Conf on Innov and Integr in Aero Sciences, 17th LTA Systems Tech Conf; followed by 2nd TEOS Forum; 2007.

[12] Sun X-Y, Li T-E, Lin G-C, Wu Y. A study on the aerodynamic characteristics of a stratospheric airship in its entire flight envelope. Proceedings of the Institution of Mechanical Engineers, Part G: Journal of Aerospace Engineering. 2018;232(5):902-21.

[13] Slotnick JP, editor Integrated CFD validation experiments for prediction of turbulent separated flows for subsonic transport aircraft. NATO Science and Technology Organization, Meeting Proceedings RDP, STO-MP-AVT-307; 2019.

[14] Yang Y, Xu X, Zhang B, Zheng W, Wang Y. Bionic design for the aerodynamic shape of a stratospheric airship. Aerospace Science and Technology. 2020; 98:105664.

[15] Manikandan M, Pant RS. Research and advancements in hybrid airships—A review. Progress in Aerospace Sciences. 2021; 127:100741.

[16] Ceruti A, Voloshin V, Marzocca P. Heuristic algorithms applied to multidisciplinary design optimization of unconventional airship configuration. Journal of Aircraft. 2014;51(6):1758-72.

[17] Liu J-m, Lu C-j, Xue L-p. Numerical investigation on the aeroelastic behavior of an airship with hull-fin configuration. Journal of Hydrodynamics, Ser B. 2010;22(2):207-13.

[18] Li Y, Nahon M, Sharf I. Airship dynamics modeling: A literature review. Progress in aerospace sciences. 2011;47(3):217-39.

[19] Wang X-L, Fu G-Y, Duan D-P, Shan X-X. Experimental investigations on aerodynamic characteristics of the ZHIYUAN-1 airship. Journal of aircraft. 2010;47(4):1463-8.

[20] Fluent A. Ansys fluent theory guide. Ansys Inc, USA. 2011; 15317:724-46.

[21] Monk D, Chadwick EA, editors. Comparison of turbulence models effectiveness for a delta wing at low Reynolds numbers. 7th European conference for aeronautics and space sciences (EUCASS); 2017. 10.13009/EUCASS2017-653

[22] Vukelich S, Williams J. The USAF Stability and Control DATCOM: Volume I, Users Manual. Tech. Rep. AFFDL-TR-79-3032 [user guide], McDonnel Douglas Astronautics; 1979.

[23] Liao L, Pasternak I. A review of airship structural research and development. Progress in Aerospace Sciences. 2009;45(4-5):83-96.

[24] Funk P, Lutz T, Wagner S. Experimental investigations on hull-fin interferences of the LOTTE airship. Aerospace Science and Technology. 2003;7(8):603-10.